

Hydrodynamic factor and effective transport coefficients for suspensions of spherical particles

Karol Makuch

21.12.2011
IPPT PAN



INNOVATIVE ECONOMY
NATIONAL COHESION STRATEGY



EUROPEAN UNION
EUROPEAN REGIONAL
DEVELOPMENT FUND

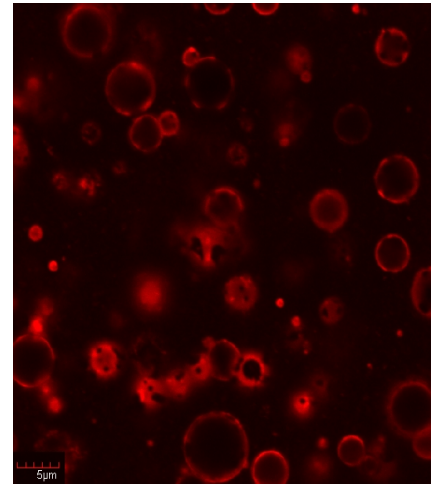


Suspensions



Macro:

Effective viscosity
Sedimentation coefficient
Hydrodynamic factor



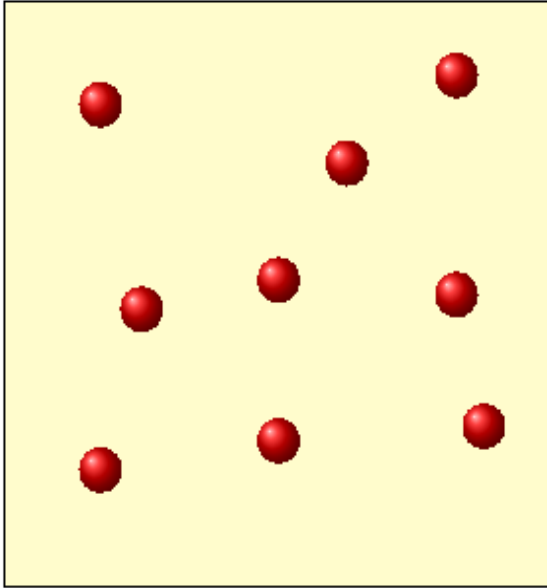
Micro:

Radius of particles
Viscosity of fluid
Number density of particles

“The simplest” system:
Suspension of spherical particles (hard spheres)
Problem: from micro to macro

Hard-sphere suspension – microscopic description

Unbounded liquid,
N particles



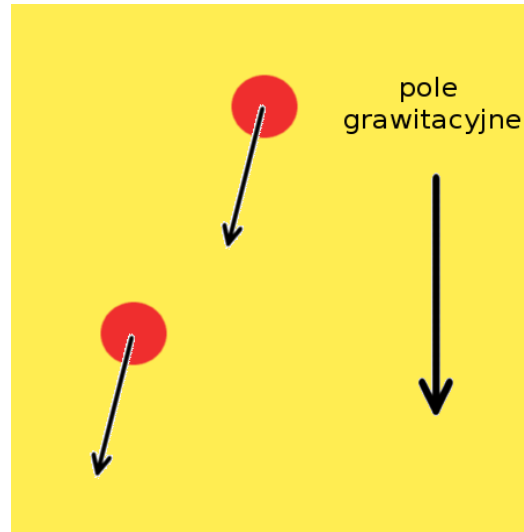
Forces acting on suspension: $\mathbf{F}_0(\mathbf{r})$ $\mathbf{F}_{\text{part}}(\mathbf{r})$
fluid particles

Response of suspension: $\mathbf{V}_i, \boldsymbol{\Omega}_i, \sum_{i=1}^N \mathbf{F}_i(\mathbf{r})$
translational and angular velocity surface forces

Stokes equations:

$$\begin{aligned} \nabla p(\mathbf{r}) - \eta \Delta \mathbf{v}(\mathbf{r}) &= \mathbf{F}_0(\mathbf{r}) + \sum_{i=1}^N \mathbf{F}_i(\mathbf{r}) \\ \nabla \cdot \mathbf{v}(\mathbf{r}) &= 0 \end{aligned}$$

Hydrodynamic interactions



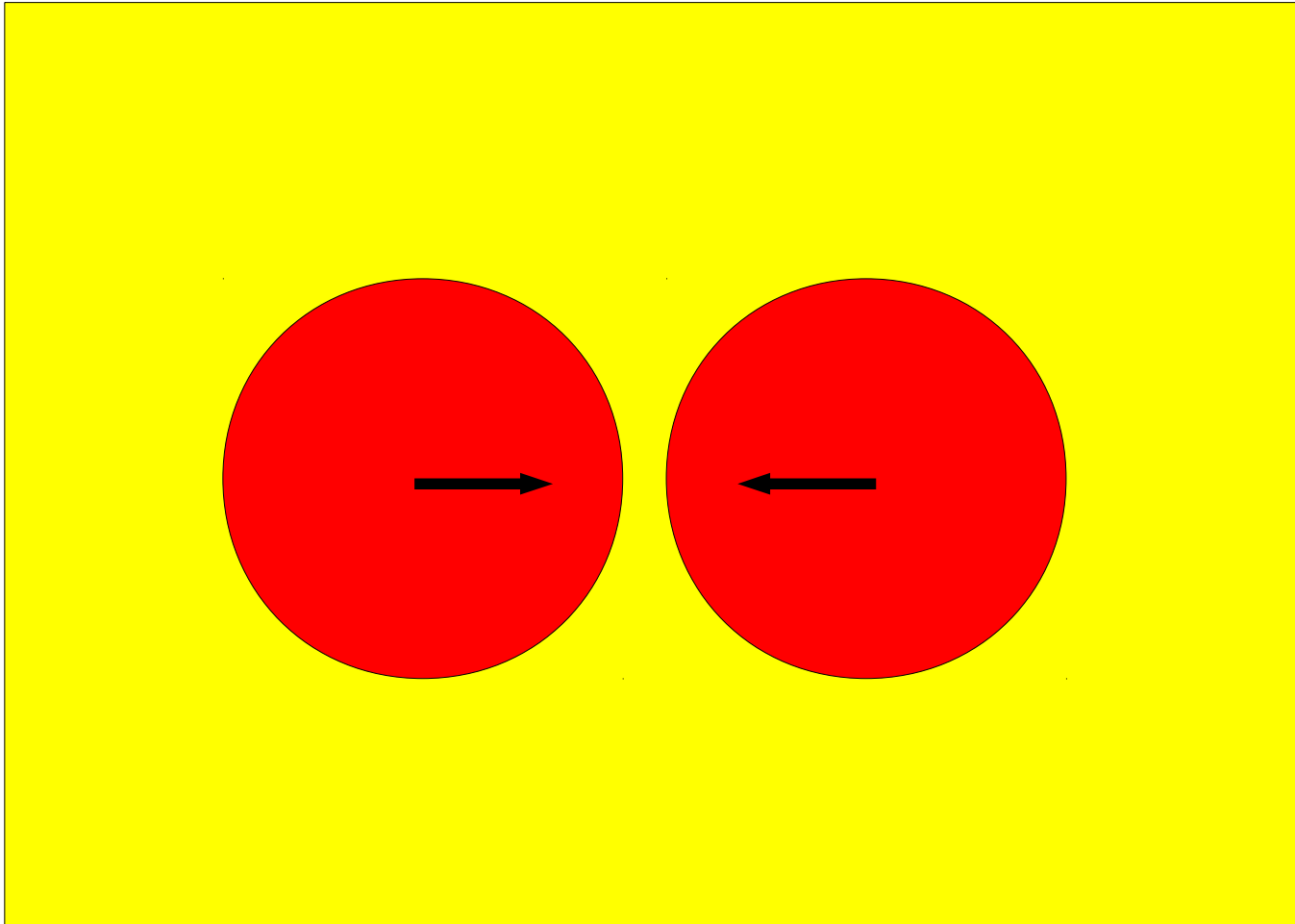
Three important features of hydrodynamic interactions:

- strong interactions of close particles
- long-range
- many-body

Hydrodynamic interactions

Strong interactions of close particles

For constant velocities asymptotically infinite drag force



Hydrodynamic interactions

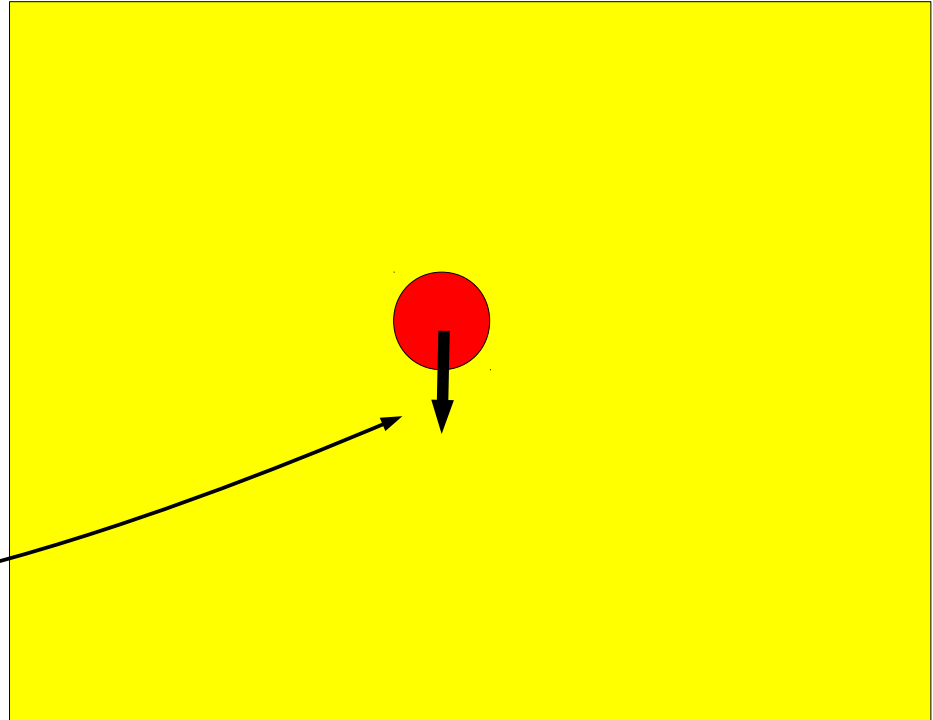
Long-range

Slow decreasing of velocity field
around sedimenting single particle

$$\mathbf{v}(\mathbf{r}) \sim \mathbf{G}(\mathbf{r}) \cdot \mathbf{F}$$

Oseen tensor:

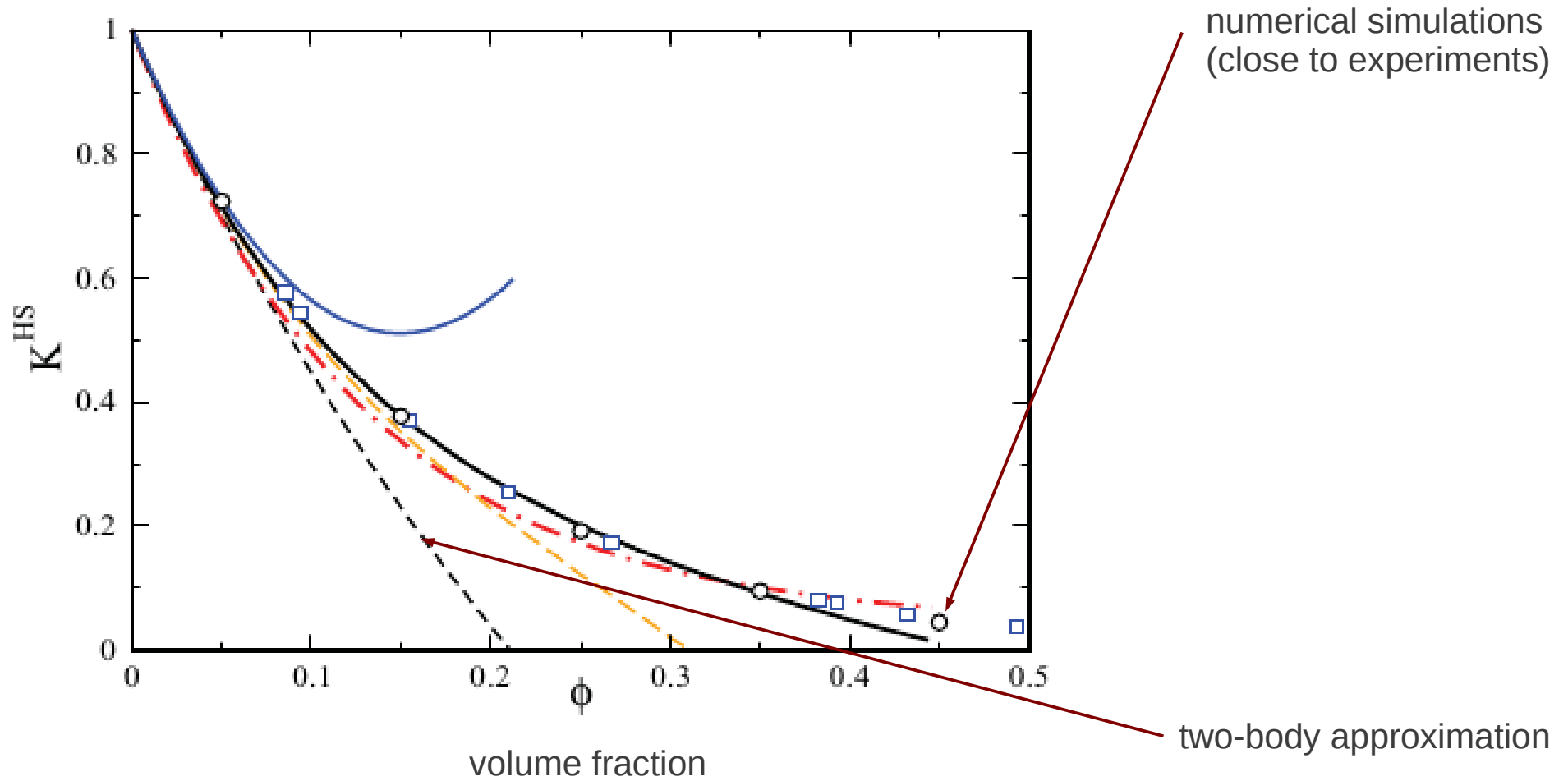
$$\mathbf{G}(\mathbf{r}) = \frac{1}{8\pi\eta} \frac{\mathbf{1} + \hat{\mathbf{r}}\hat{\mathbf{r}}}{r}$$



Hydrodynamic interactions

Many-body character

Sedimentation coefficient for hard spheres



two-body approximation relevant for volume fractions less than about 5%

Important experiment

Flow caused by force acting on particles in the area

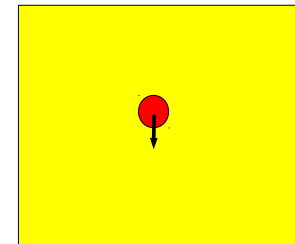
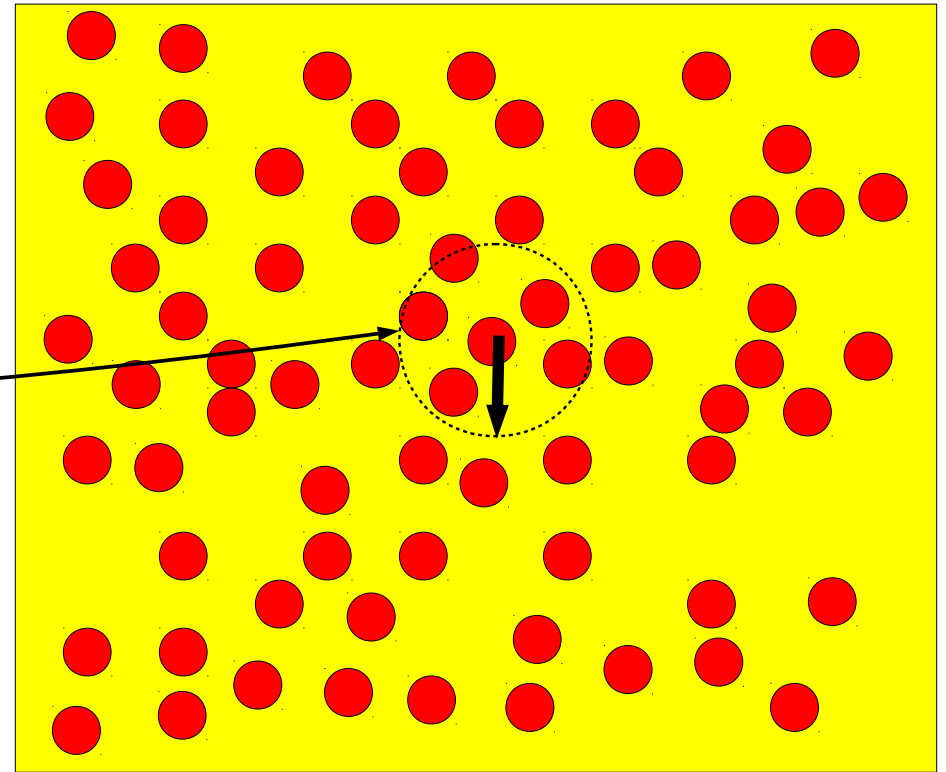
total force acting on particles in the area

$$\mathbf{v}(\mathbf{r}) \sim \mathbf{G}_{\text{eff}}(\mathbf{r}) \mathbf{F}$$

effective Green function
(effective propagator):

$$\mathbf{G}_{\text{eff}}(\mathbf{r}) \sim \frac{1}{8\pi\eta_{\text{eff}}} \frac{\mathbf{1} + \hat{\mathbf{r}}\hat{\mathbf{r}}}{r} = \frac{\eta}{\eta_{\text{eff}}} \mathbf{G}(\mathbf{r})$$

at the distance



$$\mathbf{v}(\mathbf{r}) \sim \mathbf{G}(\mathbf{r}) \cdot \mathbf{F}$$

Response of suspension (effective viscosity)

$$\langle F \rangle = T^{irr} \langle v \rangle$$

average surface force

response operator

average velocity field of suspension

Effective viscosity coefficient is given directly by the response operator T^{irr}

Renormalization

Cluster expansion (1982):

$$T^{irr} = \sum_{g=1}^{\infty} \sum_{C_1 \dots C_g} \int dC_1 \dots dC_g b(C_1 | \dots | C_g) S_I(C_1) \mathbf{G} \dots \mathbf{G} S_I(C_g)$$

block distribution function
(configurations of particles)

short-range hydrodynamic interaction

Oseen tensor (pure liquid):

$$\mathbf{G} = \frac{1}{8\pi\eta} \frac{\mathbf{1} + \hat{\mathbf{r}}\hat{\mathbf{r}}}{r}$$

Ring expansion (2011):

$$T^{irr} = \sum_{g=1}^{\infty} \sum_{C_1 \dots C_g} \int dC_1 \dots dC_g H(C_1 | \dots | C_g) S_I(C_1) \mathbf{G}_{\text{eff}} \dots \mathbf{G}_{\text{eff}} S_I(C_g)$$

block correlation function
(configurations of particles);
H=b for g=1,2,
H different from b for g>2.

Effective propagator:

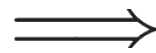
$$\mathbf{G}_{\text{eff}}(\mathbf{r}) \sim \frac{\eta}{\eta_{\text{eff}}} \mathbf{G}(\mathbf{r})$$

Two approximation schemes

Constructing approximate method by carrying over approximation from cluster expansion to ring expansion with the following modification:

$$G \Longrightarrow G_{\text{eff}}$$

Clausius-Mossotti
approximation



Generalized Clausius-Mossotti
approximation

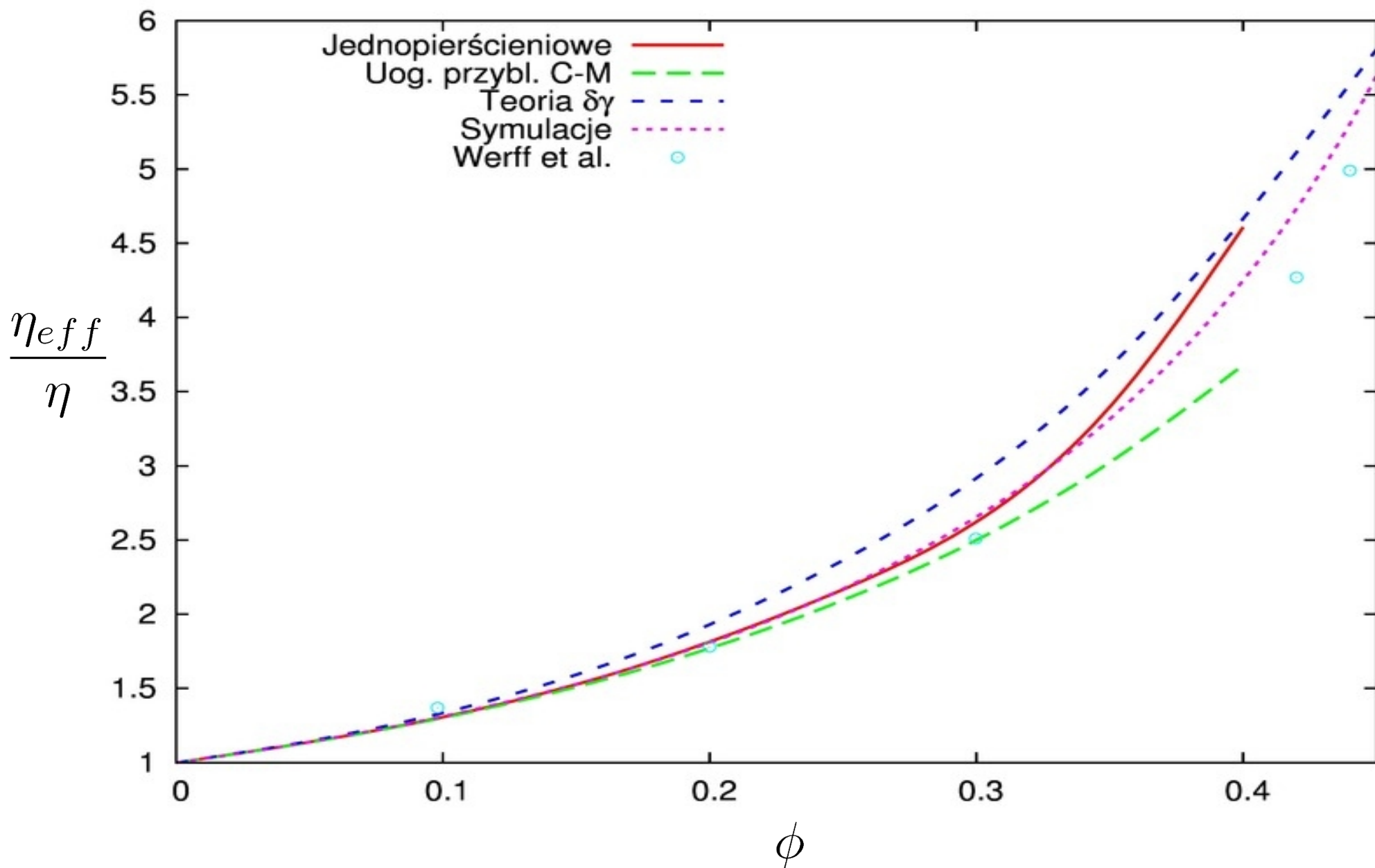
(two-body hydrodynamic interactions incomplete – the same as in $\delta\gamma$ scheme (1983))

One-ring approximation (fully takes into account two-body hydrodynamic interactions)

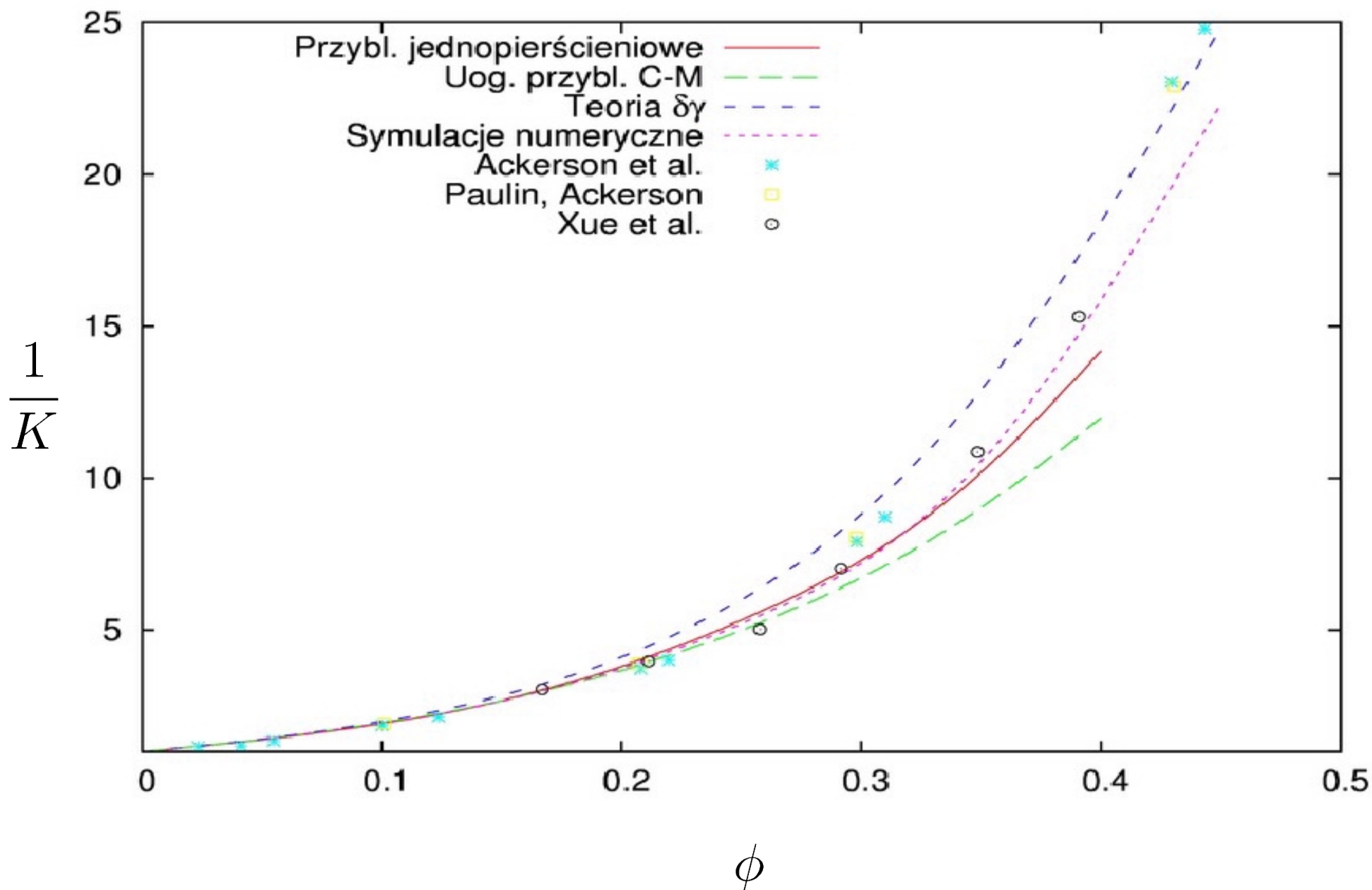
Input:

- volume fraction
- two-body correlation function (PY); (three-particle correlation function by two body correlation function (Kirkwood))
- two-body hydrodynamic interactions

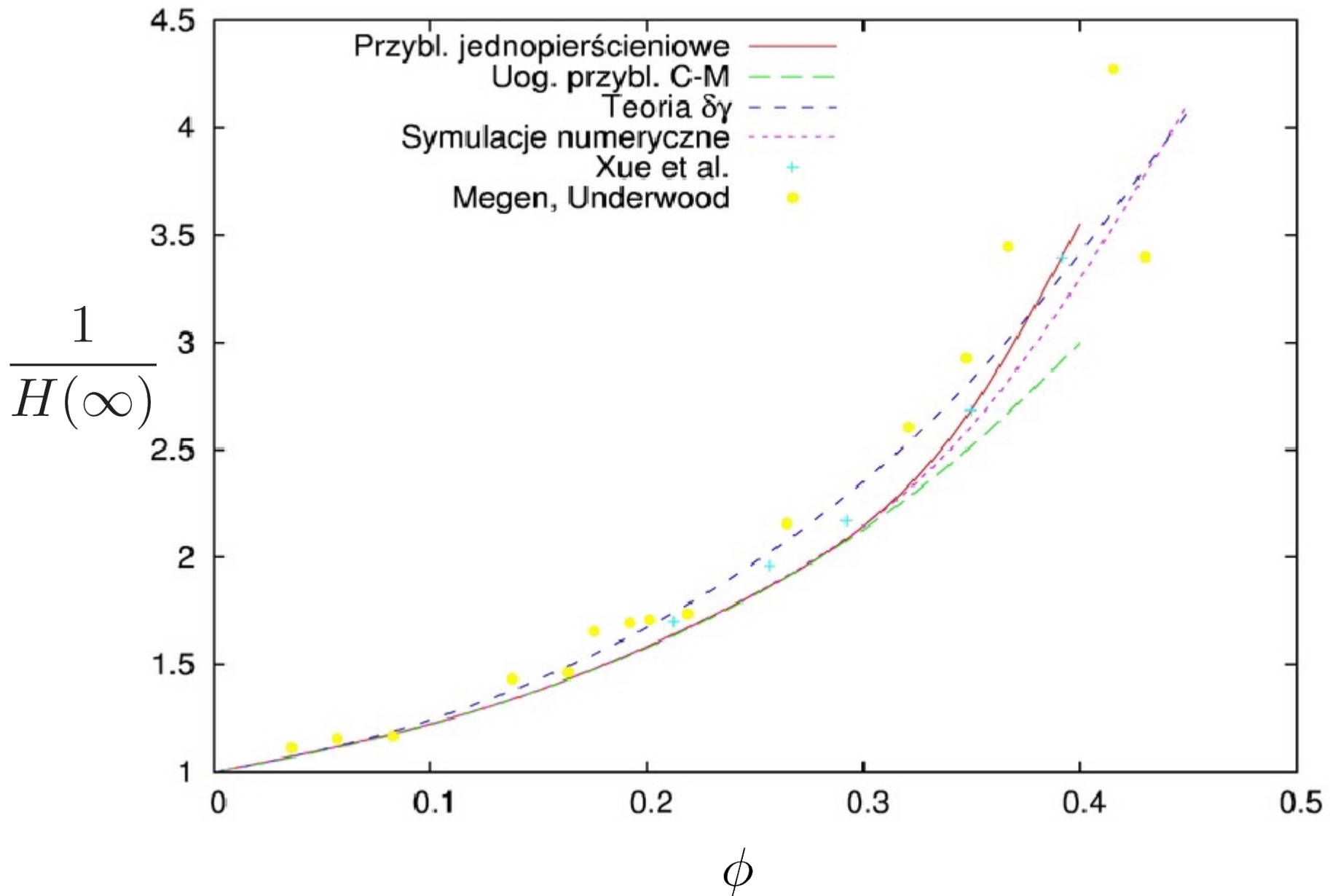
Effective viscosity



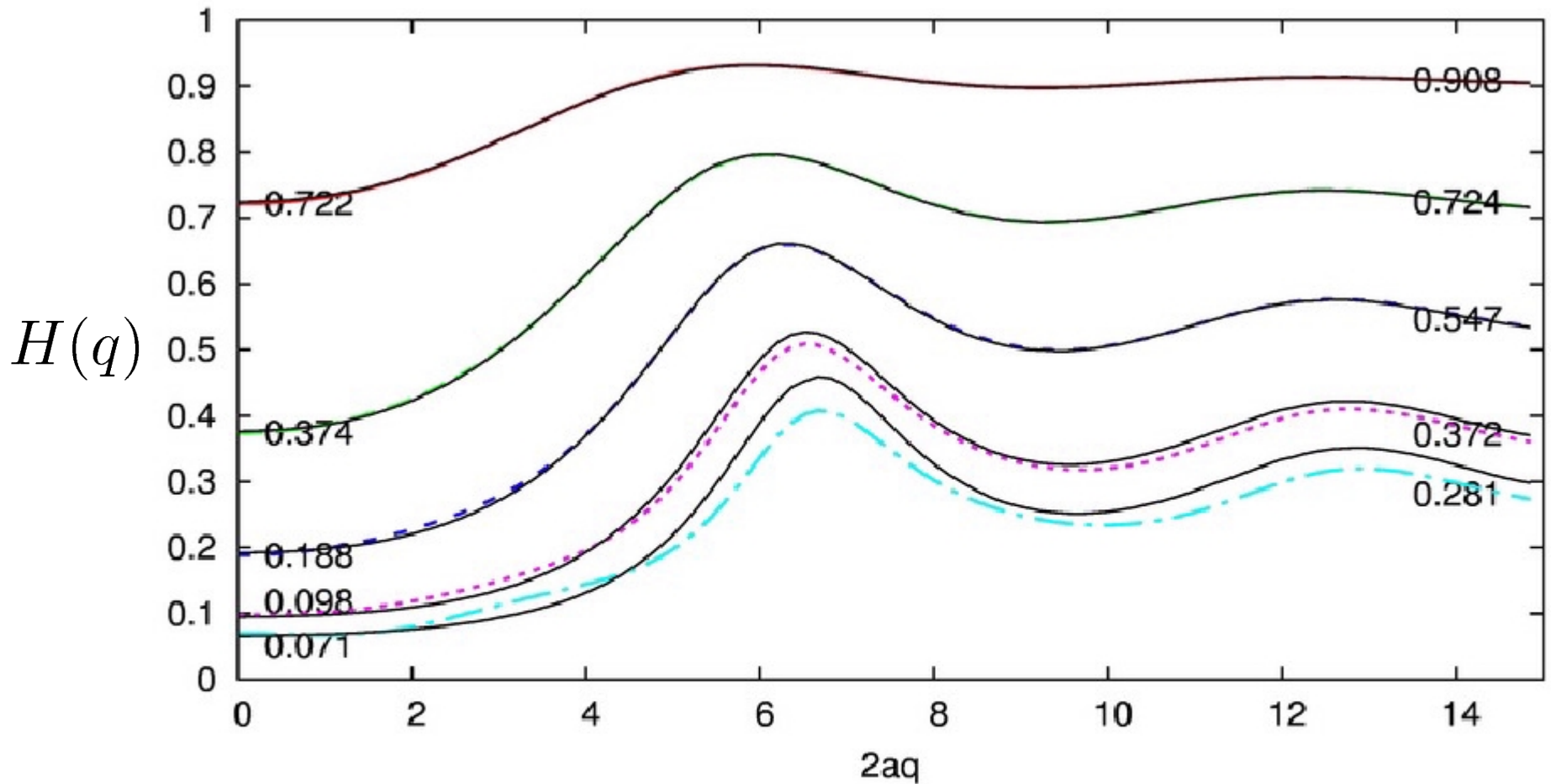
Inverse of sedimentation coefficient $K = H(0)$



Inverse of mobility of single particle in suspension $H(\infty)$



Hydrodynamic factor – one ring approximation



Jednopierścieniowe, $\phi=5\%$ ———
 Jednopierścieniowe, $\phi=15\%$ - - -
 Jednopierścieniowe, $\phi=25\%$ - - -
 Jednopierścieniowe, $\phi=35\%$ ·····
 Jednopierścieniowe, $\phi=40\%$ - · - ·

Symulacje, $\phi=5\%$ ———
 Symulacje, $\phi=15\%$ ———
 Symulacje, $\phi=25\%$ ———
 Symulacje, $\phi=35\%$ ———
 Symulacje, $\phi=40\%$ ———

Summary and possibilities

- Long-range, many-body hydrodynamic interactions and strong interactions of close particles are important in suspensions
- Ring expansion for transport coefficients – can grasp all of three above features
- Two approximation schemes for transport coefficients:
 - generalized Clausius-Mossotti approximation (two-body hydrodynamic interactions not fully taken; comparable to $\delta\gamma$ scheme),
 - **one-ring approximation** (full two-body hydrodynamic interactions, much better accuracy than hitherto theoretical methods in comparison to numerical simulations for volume fraction less than 35%)
- Simple generalization for different suspensions of spherical particles (droplets, spherical polymers) with different distributions (charged particles)

Powtarzające struktury T^{irr}

$$T^{irr} = T_{CM}^{irr} (1 - [hG] T_{CM}^{irr})^{-1}$$

Operator Clausiusa-Mossottiego

Przybliżenie Clausiusa-Mossottiego:

$$T_{CM}^{irr} \approx nM$$

$$T^{irr} = T_{RCM}^{irr} (1 - [hG_{eff}] T_{RCM}^{irr})^{-1}$$

Zrenormalizowany operator Clausiusa-Mossottiego

Uogólnione przybliżenie Clausiusa-Mossottiego:

$$T_{RCM}^{irr} \approx nB$$

Metoda przybliżona: w oparciu o przybliżone równanie na T_{RCM}^{irr}

Zrenormalizowany operator Clausiusa-Mossottiego

$$T_{RCM}^{irr} = \sum_{r=0}^{\infty} T_{RCM,r}^{irr},$$

$$T_{RCM,0}^{irr}(\mathbf{R}, \mathbf{R}') = \sum_{C_1} \int dC_1 n(C_1) S_I(C_1; \mathbf{R}, \mathbf{R}'),$$

$$T_{RCM,1}^{irr}(\mathbf{R}, \mathbf{R}') = \sum_{C_1, C_2} \int dC_1 dC_2 \int d^3\mathbf{R}_1 d^3\mathbf{R}_2 [H(C_1|C_2) - h(\mathbf{R}_1, \mathbf{R}_2)] \times \\ \times n(C_1) S_I(C_1; \mathbf{R}, \mathbf{R}_1) G_{eff}(\mathbf{R}_1, \mathbf{R}_2) n(C_2) S_I(C_2; \mathbf{R}_2, \mathbf{R}'),$$

...

Przybliżenie jednopierścieniowe

Conajwyżej jeden pierścień w T_{RCM}^{irr}

Conajwyżej dwuciałowe oddziaływania w S_I

Przybliżenie Kirkwooda na trójciałową funkcję korelacji:

$$n(123) \approx n^3 g(12) g(13) g(23)$$

Renormalizacja oddziaływań dwuciałowych:

$$S_I(12) \rightarrow BS_I(12)B$$

$$T^{irr} = nB + BT^{irr}B$$

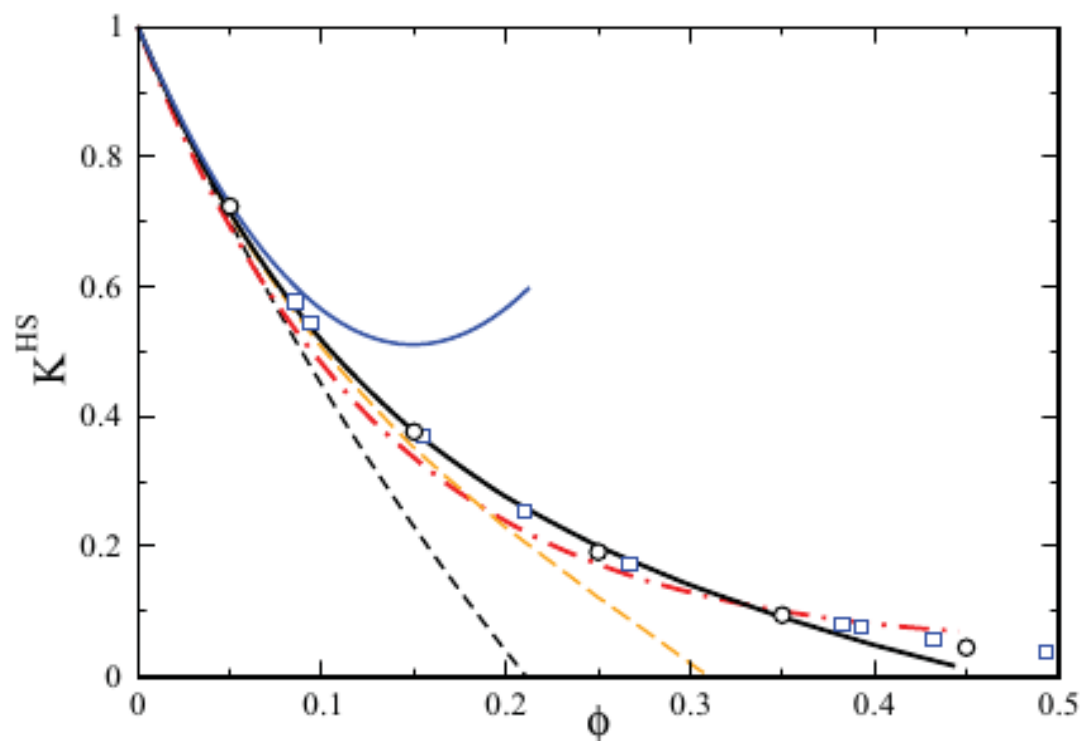


Fig. 6.3: Reduced short-time sedimentation coefficient, K^{HS} , of neutral hard spheres. Open circles: Hydrodynamic force multipole simulation data by Abade et al. [26]. Open Squares: Lattice-Boltzmann simulation data by Segrè et al. [208]. Black dashed line: PA-scheme result. Dashed-dotted red line: uncorrected $\delta\gamma$ -scheme result. Dashed orange line: self-part corrected $\delta\gamma$ -scheme result, with $d_s/d_{t,0}$ taken from the PA-scheme. Solid black line: self-part corrected $\delta\gamma$ -scheme result, with $d_s/d_{t,0}$ according to Eq. (4.26). Solid blue line: second-order virial result $K^{HS} = 1 - 6.546\phi + 21.918\phi^2$ [166]. The static structure factor input was obtained using the analytic Percus-Yevick solution.